The $[Fe(etz)_6](BF_4)_2$ Spin-Crossover System—Part Two: Hysteresis in the LIESST Regime

Roland Hinek, Hartmut Spiering, Philipp Gütlich* and Andreas Hauser*

Dedicated to Professor Karl Heinrich Lieser on the occasion of his 75th birthday

Abstract: In the $[Fe(etz)_6](BF_4)_2$ spin-crossover system the iron(II) complexes occupy two nonequivalent lattice sites, sites A and B. Complexes on site A show a thermal high-spin (HS) → low-spin (LS) transition at 105 K, whereas complexes on site B remain in the HS state down to 10 K. Complexes on both sites exhibit light-induced spin state conversions (LIESST) at 20 K: LS → HS on site A with $\lambda = 514.5$ nm, and HS → LS on site B with $\lambda = 820$ nm. The relaxation processes subsequent to the HS → LS conversion on site B reveal a light-induced HS⇌LS bistability for the complexes on site B at 70 K. The bistability as well as the absence of a thermal spin transition on site B are attributed to a thermal hysteresis for the B-site complexes with a critical temperature $T_c^{\uparrow} \approx 77$ K on heating. This hysteresis can be interpreted in terms of strong cooperative effects of elastic origin, which, in addition, cause characteristic deviations of the relaxation on site B from first-order kinetics (self-acceleration). In contrast, the HS → LS relaxation at 60 K on site A after irradiation with $\lambda = 514.5$ nm shows an unusual self-retardation.

Keywords
hysteresis · iron complexes · LIESST · spin crossover · tetrazoles

1. Introduction

The interdependence between crystal structure and spin transition behaviour of the $[Fe(etz)_6](BF_4)_2$ spin-crossover system has been reported in a preceding paper.[1] $[Fe(etz)_6](BF_4)_2$ crystallizes in the triclinic space group $P\bar{1}$ and shows two nonequivalent lattice sites, sites A and B. The site populations are $n_A:n_B = 2:1$. Complexes on site A show a thermal high-spin (HS) → low-spin (LS) transition at 105 K when the temperature is decreased, which is not quite quantitative. In contrast, the complexes on site B remain in the HS state down to 10 K. Application of an external pressure of 1200 bar did not result in any formation of the LS state on site B between 200 and 60 K. Both sites exhibit quantitative light-induced spin conversions at 20 K: LS → HS on site A and HS → LS on site B, with excitation wavelengths of 514.5 and 820 nm, respectively.

The HS⇌LS relaxation after LIESST (light-induced excited spin state trapping) is usually strongly influenced by cooperative effects, giving rise to characteristic deviations of the relaxation from first-order kinetics, as observed in the methyl and propyl derivatives.[2, 3] Cooperative effects arise through elastic interactions between the complex molecules during the spin transition,[4, 5] due to the large difference in bond length between the HS and LS states of about 0.2 Å.[6, 7] In a simple model their influence can be pictured as an internal pressure acting on the HS and LS states in much the same way as an external pressure.[8] This internal pressure increases with increasing LS fraction γ_{LS}, which results in a shift in both horizontal and vertical displacements of the HS and LS potential wells relative to each other, as shown schematically in Figure 1.[9] The latter is the dominant effect, giving rise to a substantial increase in the zero-point energy difference ΔE^0_{HL}. For the methyl and propyl systems of the $[Fe(Rtz)_6](BF_4)_2$ series it was possible to estimate the vertical shifts of the potential wells from the observed shifts in the energy of the $^1A_1 - {}^1T_1$ d–d bands during the HS → LS relaxation. It was found to depend linearly on the actual LS concentration γ_{LS} during the relaxation with a slope on the order of 100–200 cm^{-1}.[2, 9]

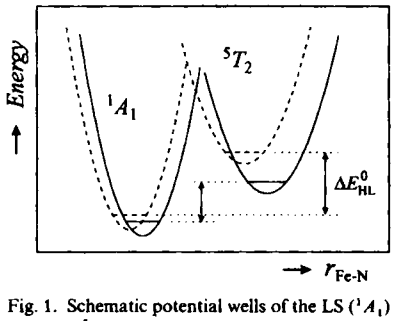

Fig. 1. Schematic potential wells of the LS ($^1A_1$) and HS ($^5T_2$) states at different overall LS concentrations γ_{LS} in the crystal. Solid lines: $\gamma_{LS} = 0$. Broken lines: $\gamma_{LS} = 1$. There is a substantial increase in the zero-point energy difference ΔE_{HL} with γ_{LS} due to the increased internal pressure in the crystal.

In this second report on $[Fe(etz)_6](BF_4)_2$, a detailed study of the relaxation processes after LIESST on the two sites is pre-

[*] A. Hauser
Institut für Anorganische, Analytische und Physikalische Chemie
Universität Bern, Freiestrasse 3, CH-3000 Bern (Switzerland)
Fax: Int. code +(31)65-3993
e-mail: ahauser@iac.unibe.ch
P. Gütlich, R. Hinek, H. Spiering
Institut für Anorganische Chemie und Analytische Chemie
Universität Mainz, Staudingerweg 9, D-55099 Mainz (Germany)
Fax: Int. code +(6131)39-2990
e-mail: guetlich@dacmza.chemie.uni-mainz.de

sented. Special attention is paid to cooperative effects, which manifest themselves in characteristic deviations from first-order kinetics on site B. In addition, the cooperative effects are suggested to be strong enough to cause an unusual light-induced HS⇌LS bistability on site B at 70 K. The bistability is the main subject of this work.

2. Results

2.1. Narrow-Band Irradiation with $\lambda = 514.5$ nm (LIESST): The optical single-crystal absorption spectra of $[Fe(etz)_6](BF_4)_2$ were recorded at 60 K, at time intervals of 500 s following irradiation with 514.5 nm. Figure 2 visualizes the time dependence of the HS → LS relaxation process on site A. From the basic kinetic data of Figure 2, the HS → LS relaxation curve and the corresponding rate constant k_{HL} have been derived as a function of the relaxation time t, as shown in Figure 3a and 3b, respectively. At short times, the relaxation is self-accelerating (region 1 of Fig. 3a), corresponding to the initial increase of the rate constant in Figure 3b. Above a value of $\gamma_{LS} \approx 0.3$, that is, for $t \geq 6000$ s, the rate constant begins to drop, now giving rise to a pronounced self-retardation (region 2 of Fig. 3a).

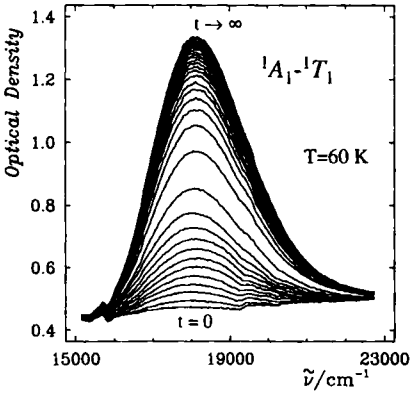

Fig. 2. Recovery of the $^1A_1-^1T_1$ absorption band (LS band) during the HS → LS relaxation on site A at 60 K after irradiation with 514.5 nm. The time interval is between measurements is 500 s.

The $^1A_1-^1T_1$ transition energy depends in a complicated way upon the relaxation time (see Fig. 3c), and, in contrast to the mtz and ptz systems,[2, 9] it no longer depends linearly on γ_{LS}. In region 2 the $^1A_1-^1T_1$ transition energy is nearly constant.

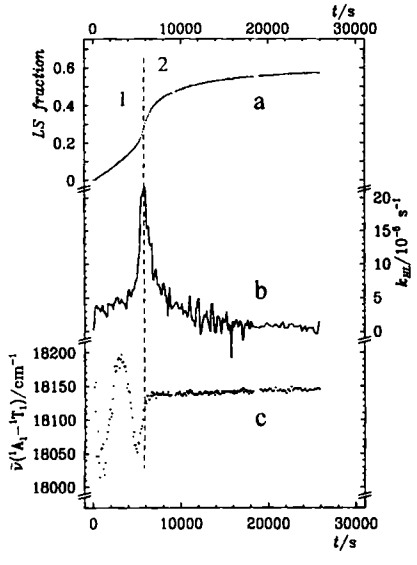

Fig. 3. a) HS → LS relaxation curve of $[Fe(etz)_6](BF_4)_2$ following irradiation with $\lambda = 514.5$ nm at $T = 60$ K, b) rate constant k_{HL}, and c) $^1A_1-^1T_1$ transition energy. All data derived from the optical relaxation spectra shown in Fig. 2.

2.2. Narrow-Band Irradiation with $\lambda = 820$ nm (Reverse LIESST): Figure 4 shows optical absorption spectra of $[Fe(etz)_6](BF_4)_2$ before and after narrow-band irradiation at $\lambda = 820$ nm. Spectra a and b characterize the thermal spin equilibrium on site A at 80 and 70 K, respectively, before irradiation. Spectrum c was recorded directly after irradiation at 70 K. It shows an overall increase in singlet intensity. From the previous Mössbauer study it is known that this is basically due to the light-induced HS → LS conversion on site B, but that there is a small residual quintet intensity because of a small steady-state HS concentration on site A.[11] The latter is due to the spectral overlap of the spin-forbidden $^1A_1-^3T_1$ and $^1A_1-^3T_2$ transitions of the LS species and the spin-allowed $^5T_2-^5E$ transition of the HS species.[10] After equilibration at 70 K, spectrum d was measured within a few minutes. Quite unexpectedly it shows the full singlet intensity and no longer any quintet intensity; this indicates that the steady-state HS concentration of around 10% on site A, still present in spectrum c, has decayed completely within a HS → LS relaxation. This relaxation is denoted as type I relaxation.

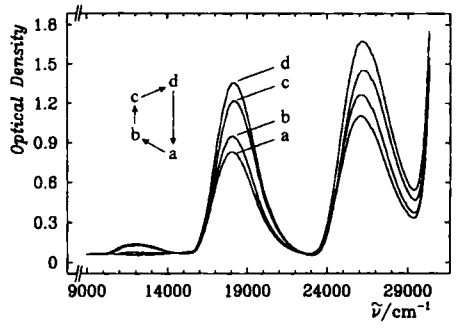

Fig. 4. UV/Vis/NIR absorption spectra of $[Fe(etz)_6](BF_4)_2$. The band at 12000 cm^{-1} originates from the $^5T_2-^5E$ transition (HS band), those at 18000 and 26000 cm^{-1} arise from the $^1A_1-^1T_1$ and $^1A_1-^1T_2$ transitions (LS bands), respectively: a) 80 K, before irradiation and after irradiation and relaxation (equilibrium); b) 70 K, before irradiation (equilibrium); c) 70 K, directly after irradiation with 820 nm (nonequilibrium); d) 70 K after irradiation with 820 nm and relaxation (equilibrium).

Figure 5 shows corresponding relaxation curves for type I relaxation at different temperatures together with exponential fits. Within the accessible temperature range $56 > T > 72$ K the dependence of the rate constant follows an Arrhenius-type be-

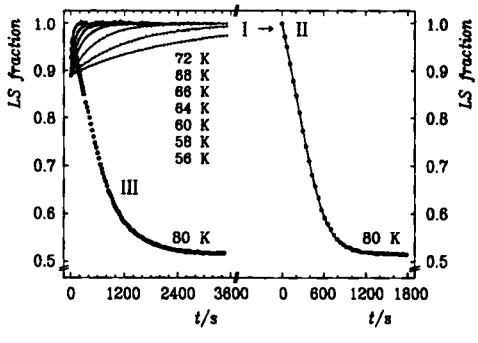

Fig. 5. Different relaxation curves found after irradiation at 820 nm, derived from optical data. Type I: HS → LS relaxation on site A at $T \leq 72$ K; type II: LS → HS relaxation on sites A and B at $T = 80$ K, after preparation of the sample in the LS state at 56 K and subsequent heating to 80 K; type III: initial HS → LS relaxation on site A and subsequent LS → HS relaxation on site B at $T = 80$ K, after warming directly from 20 to 80 K. A critical temperature T_c ($72 < T_c < 80$ K) exists below which bistability is observed (see text).

0947-6539/96/0211-1436 $ 15.00+.25/0 Chem. Eur. J. 1996, 2, No. 11

haviour (Fig. 6). A linear regression gives a frequency factor $A \approx 35000\ s^{-1}$ and an activation energy $E^*_{HL} \approx 700\ cm^{-1}$ for the HS → LS relaxation of the residual HS(A) fraction.

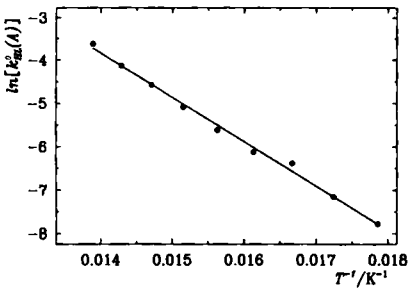

Fig. 6. Arrhenius-plot of the rate constant after irradiation at 820 nm of type I relaxation between 56 and 72 K.

At 70 K the full singlet intensity of spectrum d in Figure 4 remains absolutely stable. However, upon fast warming from 70 to 80 K it becomes unstable, and an abrupt LS → HS relaxation at 80 K results, denoted as type II relaxation in Figure 5. It deviates strongly from first-order kinetics. In contrast to type I relaxation, type II relaxation shows a noticeable dependence of the rate constant on γ_{LS}. The latter is shown in Figure 5 together with a numerical fit, according to expression (1) for the rate

$$k_{LH}(\gamma_{HS}) = k_0 \exp(\alpha \gamma_{HS}) \quad (1)$$

constant,[12] where $k_0 = 1.50(1) \times 10^{-3}\ s^{-1}$ and the self-acceleration parameter $a = 1.42(7)$. The absorption spectrum obtained at 80 K following type II relaxation is identical to the one obtained in thermal equilibrium before irradiation at 80 K (Fig. 4, spectrum a): all site B complexes are in the HS state, and a portion of the complexes are in the HS state on site A, according to the thermal spin transition on the latter. Thus, type II relaxation must be regarded as the superposition of mainly LS(B) → HS(B) relaxation and some LS(A) → HS(A) relaxation. On cooling from 80 to 70 K one never returns to spectrum d of Figure 4, but again to the equilibrium spectrum b. The cycle a → b → c → d → a in Figure 4 can be repeated over and over again.

In addition to the relaxation types I and II, a third type of relaxation behaviour occurs when the sample is warmed up to 80 K directly after irradiation (Fig. 5, relaxation III). Clearly, its unusual appearance is due to a superposition of opposite directions of relaxation on the two sites, namely, comparatively fast HS(A) → LS(A) and subsequent slower LS(B) → HS(B) relaxation. Nevertheless, the spin equilibria following type II and III relaxations at 80 K are the same.

Spectra b and d in Figure 4 demonstrate the existence of a light-induced HS(B)⇌LS(B) bistability in $[Fe(etz)_6](BF_4)_2$. This is the most important result of this paper. From Figure 5 a critical temperature T_c of $72 < T_c < 80$ K can be deduced, below which bistability is observed. T_c can be derived with more accuracy by stepwise warming from 20 K after irradiation with 820 nm. Type I relaxation then sets in at 56 K, with the appearance of full singlet spectra at 56 K. On further warming in steps of 2 K, a sharp spin transition occurs at $T_c \approx 77$ K, as shown in Figure 7. At 80 K, the corresponding transition curve joins up with the one obtained before irradiation, which corresponds to the spin transition on site A only, with $T_{1/2} = 105$ K. In fact, on decreasing the temperature from 80 to 50 K again, the same behaviour as before irradiation is found. Thus, the sharp spin

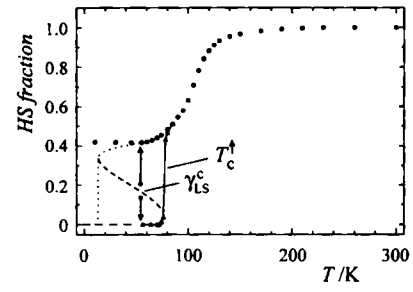

Fig. 7. Spin transitions in $[Fe(etz)_6](BF_4)_2$ on the two sites: thermal spin transition on site A without hysteresis (o) and thermal spin transition on site B after irradiation with 820 nm and subsequent heating in steps (▲). The spin transition on site B occurs at $T_c \approx 77$ K, which is identified as $T_c^{\uparrow}$ of the heating branch of a hysteresis loop. The arrows indicate relaxation processes possible inside the hysteresis subsequent to irradiation. The relaxation direction inside the hysteresis is determined by the existence of a critical LS concentration γ_{LS}^c at given temperature, as visualized by the sigmoidal curve inside the loop.

transition at $T_c \approx 77$ K on site B after irradiation is observable only on heating.

2.3. Broad-Band Irradiation: In addition to the critical temperature T_c, there is a critical LS fraction γ_{LS}^c characteristic for the bistable behaviour on site B. For $T < T_c$ and $\gamma_{LS} < \gamma_{LS}^c$ relaxation towards $\gamma_{LS} = 0.58$, as observed in the normal cooling mode, and for $\gamma_{LS} > \gamma_{LS}^c$ relaxation towards $\gamma_{LS} = 1$ are expected to occur. In order to determine γ_{LS}^c, relaxation experiments at $T < T_c$ with broad-band irradiation were performed. With different cut-off filters, different steady-state LS concentrations as starting concentrations $\gamma_{LS}(t = 0)$ for subsequent relaxation processes can be created. In Figure 8 these starting concentrations to-

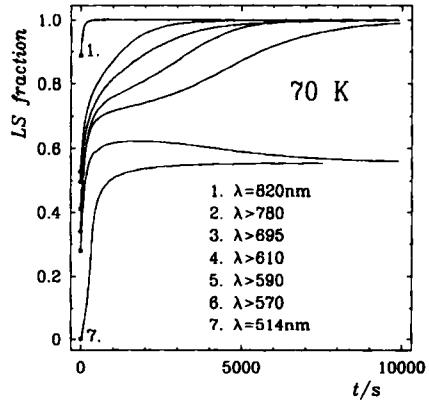

Fig. 8. Optical HS → LS relaxation curves at 70 K after different broad-band irradiation conditions starting from different total LS concentrations (•). At 70 K a critical total LS concentration γ_{LS}^c of between 0.28 and 0.34 exists for the B-site complexes.

gether with their respective relaxation curves at 70 K are shown. The values for $\gamma_{LS}(t = 0)$ decrease on going to shorter irradiation wavelengths, because of the increasing spectral overlap of the excitant light with the $^1A_1 - {}^1T_1$ absorption band. For comparison, the relaxation curves following narrow-band irradiation with 514.5 nm ($\gamma_{LS}(t = 0) = 0$) and 820 nm ($\gamma_{LS}(t = 0) = 0.89$) are included. For $\gamma_{LS}(t = 0) > 0.3$, the LS fraction tends towards $\gamma_{LS}(t \to \infty) = 1$; for $\gamma_{LS}(t = 0) < 0.3$, it tends towards $\gamma_{LS}(t \to \infty) = 0.56$. This is, as expected, equal to the value of 0.56 from the thermal transition curve.[11] The critical value for the LS fraction is $\gamma_{LS}^c \approx 0.3$.

The unusual appearance of the curves in Figure 8 is due to a superposition of the simultaneous relaxation processes on the

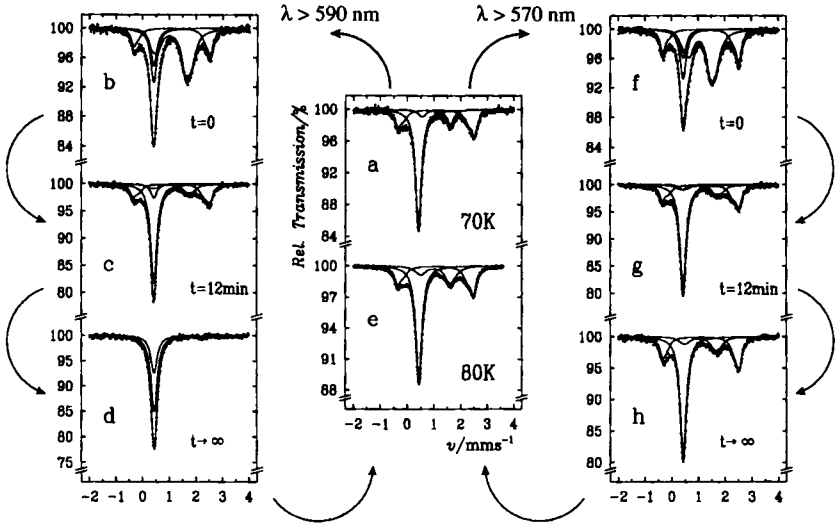

Fig. 9. ^{57}Fe Mössbauer spectra of $[Fe(etz)_6](BF_4)_2$ recorded at different temperatures before and after broad-band irradiation with $\lambda > 570$ nm and $\lambda > 590$ nm: a) 70 K, before irradiation (equilibrium). b) 20 K, after irradiation with $\lambda > 590$ nm; corresponds to the system directly after irradiation with $\lambda > 590$ nm at 70 K, i.e., to the relaxation at $t = 0$ and 70 K. c) 20 K, after the sample was heated up to 70 K for 12 min and subsequently brought back down to 20 K. d) 20 K, after the sample equilibrated completely at 70 K ($t \rightarrow \infty$) and was brought back to 20 K. e) 80 K, before and after irradiation (equilibrium). f) 20 K, after irradiation with $\lambda > 570$ nm; corresponds to the system directly after irradiation with $\lambda > 570$ nm at 70 K, i.e., to the relaxation at $t = 0$ and 70 K. g) 20 K, after the sample was heated up to 70 K for 12 min and subsequently brought back down to 20 K. h) 20 K, after the sample equilibrated completely at 70 K ($t \rightarrow \infty$) and was brought back to 20 K.

two sites. Since the two relaxation processes cannot be resolved from each other by using optical spectroscopy, a detailed Mössbauer study of the most interesting relaxation curves of Figure 8 was carried out, namely, of curves 5 and 6. The results are shown in Figure 9. The parameters of the Mössbauer spectra are collected in Table 1.

Spectrum a of Figure 9 is the normal Mössbauer spectrum of $[Fe(etz)_6](BF_4)_2$ in thermal equilibrium at 70 K. Spectra b and f were recorded at 20 K immediately following irradiation with $\lambda > 590$ and 570 nm, respectively. At 20 K all relaxation processes are extremely slow; only at $T > 50$ K do thermally activated processes set in. In fact, at 70 K the HS⇌LS relaxation is somewhat too fast to allow a simple consecutive recording of Mössbauer spectra, but the relaxation is sufficiently slow to allow temperature quenching of the system at any stage of the relaxation by rapidly cooling the sample down to 20 K. Thus, spectra c and g were also recorded at 20 K, but after the samples had been maintained at 70 K for 12 minutes, to allow relaxation processes to take place, before being cooled back to 20 K. In the left- and right-hand columns of Figure 9 there is an initial comparatively fast increase in intensity of the LS(A) resonance and a slow decrease of the LS(B) resonance. For $\lambda > 570$ nm, this leads to the final spectrum with all complexes on site B and only a small residual fraction of complexes on site A in the HS state. In fact, the corresponding spectrum h is identical to the spectrum before irradiation. For $\lambda > 590$ nm, which starts off with a slightly higher total LS fraction (see Table 1), however, the initial decrease in the LS(B) resonance is reversed at some stage, and the sample ends up with all complexes on both sites in the LS state. This is in accordance with the relaxation curves 5 and 6 of Figure 8.

3. Discussion

The cooperative effects due to elastic interactions between the complexes in the crystal can be pictured in a very oversimplified way as being the result of an internal pressure acting upon the

Table 1. ^{57}Fe Mössbauer parameters of the HS⇌LS relaxation processes subsequent to broad-band irradiation experiments in $[Fe(etz)_6](BF_4)_2$ [a].
a) Broad-band irradiation with $\lambda > 590$ nm.

	HS(A)				HS(B)				LS(A)				LS(B)			
t [min]	ΔE_Q [mms^{-1}]	δ_{iso} [mms^{-1}]	$\Gamma_{1/2}$ [mms^{-1}]	γ_{HS}	ΔE_Q [mms^{-1}]	δ_{iso} [mms^{-1}]	$\Gamma_{1/2}$ [mms^{-1}]	γ_{HS}	ΔE_Q [mms^{-1}]	δ_{iso} [mms^{-1}]	$\Gamma_{1/2}$ [mms^{-1}]	γ_{LS}	ΔE_Q [mms^{-1}]	δ_{iso} [mms^{-1}]	$\Gamma_{1/2}$ [mms^{-1}]	γ_{LS}
0	1.01(2)	1.08*	0.16*	0.47	2.54(9)	1.100(8)	0.18*	0.20	–	0.422*	0.14*	0.20	–	0.422*	0.14*	0.14
	1.43(3)		0.22*		2.87(3)		0.12*									
≈12	1.10(8)	1.08*	0.16*	0.13	2.45(4)	1.090(6)	0.18*	0.26	–	0.432(1)	0.14*	0.53	–	0.432*	0.14*	0.08
	1.57(10)		0.22*		2.89(2)		0.12*									
≈30	1.15(9)	1.08*	0.16*	0.12	2.53(7)	1.093(9)	0.18*	0.19	–	0.434(1)	0.14*	0.55	–	0.433*	0.14*	0.14
	1.74(10)		0.22*		2.92(3)		0.12*									
≈120	1.05(15)	1.08*	0.16*	0.08	2.44(11)	1.09(2)	0.18*	0.13	–	0.434(2)	0.14*	0.59	–	0.434*	0.14*	0.20
	1.58(22)		0.22*		2.89(5)		0.12*									
≈600	1.02(22)	1.08*	0.16*	0.05	2.39(27)	1.09(2)	0.18*	0.08	–	0.437(1)	0.14*	0.61	–	0.437*	0.14*	0.25
	1.57(33)		0.22*		2.84(6)		0.12*									
>1800	–	–	–	–	–	–	–	–	–	0.442*	0.15*	0.66	–	0.442*	0.15*	0.33

b) Broad-band irradiation with $\lambda > 570$ nm.

	HS(A)				HS(B)				LS(A)				LS(B)			
t [min]	ΔE_Q [mms^{-1}]	δ_{iso} [mms^{-1}]	$\Gamma_{1/2}$ [mms^{-1}]	γ_{HS}	ΔE_Q [mms^{-1}]	δ_{iso} [mms^{-1}]	$\Gamma_{1/2}$ [mms^{-1}]	γ_{HS}	ΔE_Q [mms^{-1}]	δ_{iso} [mms^{-1}]	$\Gamma_{1/2}$ [mms^{-1}]	γ_{LS}	ΔE_Q [mms^{-1}]	δ_{iso} [mms^{-1}]	$\Gamma_{1/2}$ [mms^{-1}]	γ_{LS}
0	0.76(2)	1.08*	0.16*	0.48	2.41(7)	1.099(5)	0.18*	0.24	–	0.438*	0.14*	0.18	–	0.438*	0.14*	0.10
	1.15(3)		0.22*		2.87(1)		0.12*									
≈12	1.06(7)	1.08*	0.16*	0.14	2.41(4)	1.097(6)	0.18*	0.29	–	0.431*	0.14*	0.54	–	0.431*	0.14*	0.03
	1.54(9)		0.22*		2.88(1)		0.12*									
>1800	1.01(9)	1.08*	0.16*	0.16	2.58(5)	1.096(5)	0.18*	0.30	–	0.432*	0.14*	0.54	–	0.432*	0.14*	0
	1.35(11)		0.22*		2.87(2)		0.12*									

[a] Asterisks denote fixed parameters. The two values for parameters ΔE_Q and $\Gamma_{1/2}$ of the HS species are due to the line broadening (see ref. [1]).

0947-6539/96/0211-1438 $ 15.00+.25/0 Chem. Eur. J. 1996, 2, No. 11

individual complexes in much the same way as an external pressure. The LS state, having a markedly smaller volume than the HS state, is stabilized by both an external and an internal pressure.[8, 9] Thus, in this simplified picture, because the internal pressure increases with the number of complexes in the LS state, cooperative effects tend to stabilize the dominant species. This is the basic reason for the self-accelerating relaxation curves often observed in neat spin-crossover compounds. If the value of the so-called interaction constant is larger than a critical value, elastic interactions also lead to hysteresis behaviour in the spin transition without any accompanying crystallographic phase transitions.[5, 11]

The light-induced bistability on site B may be interpreted qualitatively on this basis. At room temperature, with all complexes in the HS state, the quantum mechanical ground state of site A complexes is still the LS state, but only populated to a negligible extent because of its low density of states. As the temperature is lowered, complexes on site A relax to the LS state. This, in turn, stabilizes the LS state and the positive feedback results in a comparatively steep transition curve for site A. It is reversible, the interaction constant not being sufficiently large for a hysteresis to occur. For site B complexes the quantum mechanical ground state at room temperature is the HS state, and it remains so down to below 50 K, even though the spin transition on site A stabilizes the LS state on both sites. However, the zero-point energy difference between HS and LS for site B complexes is very close to zero at this stage. The additional stabilization achieved by the partial light-induced population of the LS state on site B is sufficient to result in a crossover of the quantum mechanical ground state of the site B complexes from the HS to the LS state. That this is really the case is borne out by the relaxation curves of Figure 8 with the critical value for $\gamma_{LS}^{C}(t = 0) \approx 0.3$. For $\gamma_{LS}(t = 0) > 0.3$, the LS state on site B is the true ground state and the relaxation proceeds towards $\gamma_{LS}(t \rightarrow \infty) = 1$.

The critical temperature T_c of around 77 K in the heating mode following the preparation of the sample in the pure LS state on both sites is thus the thermodynamic transition temperature $T_c^{\uparrow} \approx$ of a spin transition with a hysteresis on site B. The corresponding branch of the hysteresis in cooling mode is not accessible in a simple temperature cycle. It is either well below 50 K, at a temperature for which the HS → LS relaxation is negligibly slow, or the HS state is indeed still the true ground state. The, at first sight, rather complex relaxation behaviour is now fairly straightforward to explain as a relaxation process starting from values for $\gamma_{LS}(t = 0)$ and T within or outside the hysteresis. As mentioned above, irradiation into the $^5T_2 - {}^5E$ band of the Rtz series of spin-crossover compounds usually does not lead to a quantitative light-induced HS → LS conversion. Rather, a steady-state type situation with a typical steady-state LS fraction of approximately 86% results,[1] owing to the spectral overlap of HS and LS absorption bands in that region. This is true for the A-site complexes in $[Fe(etz)_6](BF_4)_2$, but interestingly, the light-induced HS → LS conversion on site B is quantitative. This indicates that the quantum efficiencies of the various intersystem crossing steps involved depend sensitively upon the exact molecular geometry dictated by the second coordination sphere or the crystal lattice.[10]

The self-retardation in the later stages of the straightforward HS → LS relaxation on site A (region 2 in Fig. 3) could have two possible explanations:

1) It could be correlated to the disordered crystal structure and the rather large inhomogeneous distribution of zero-point energy differences, similar to the behaviour found for spin-crossover complexes in polymer matrices.[12]
2) The HS → LS relaxation could be nonstatistical with nearest-neighbour correlations of an "antiferromagnetic" type.[13]

In view of the fact that the peak position of the $^1A_1 - {}^1T_1$ band behaves rather erratically during the relaxation, in contrast to ptz and mtz, the former explanation is more likely. In fact a large inhomogeneous distribution of zero-point energies would also explain the residual HS fraction on site A at 10 K.

The characteristic features of the $[Fe(etz)_6](BF_4)_2$ spin-crossover system are the absence of a thermal spin transition as well as the presence of a light-induced bistability for the complexes on site B. This can be understood in terms of a hysteresis behaviour for the B-site complexes, where the hysteresis is due to strong cooperative effects of elastic origin. In order to definitely rule out the possibility that an ordinary crystallographic phase transition after irradiation is due to the light-induced bistability, it is very desirable to carry out crystal structure determinations after irradiation at low temperature. In addition, heat capacity measurements during the relaxation processes after irradiation could answer the question about the "true ground state" for the complexes on site B before and after irradiation.

4. Experimental Procedure

The experimental procedures used in this paper have been described in Section 5 of the previous paper in this issue (ref. [1]).

Acknowledgement: We wish to thank the Deutsche Forschungsgemeinschaft, the Schweizerische National Fonds, the Fonds der Chemischen Industrie, the Materialwissenschaftliches Forschungszentrum der Universität Mainz and the European Community (Network Contract No. ERB CHRX CT92 0080) for financial support of this work.

Received: March 15, 1996 [F323]

[1] R. Hinek, H. Spiering, D. Schollmeyer, P. Gütlich, A. Hauser, *Chem. Eur. J.* **1996**, *2*, 1427–1434.
[2] R. Hinek, P. Gütlich, A. Hauser, *Inorg. Chem.* **1994**, *33*, 567–572.
[3] A. Hauser, P. Gütlich, H. Spiering, *Inorg. Chem.* **1986**, *25*, 4245–4248.
[4] H. Spiering, E. Meissner, H. Köppen, E. W. Müller, P. Gütlich, *Chem. Phys.* **1982**, *68*, 65–71.
[5] L. Wiehl, G. Kiel, C. P. Köhler, H. Spiering, P. Gütlich, *Inorg. Chem.* **1986**, *25*, 1565–1571.
[6] L. Wiehl, H. Spiering, P. Gütlich, K. Knorr, *J. Appl. Crystallogr.* **1990**, *23*, 151–160.
[7] L. Wiehl, *Acta Crystallogr. Sect. B* **1993**, *49*, 289–303.
[8] H. G. Drickamer, C. W. Frank, *Electronic Transitions and the High Pressure Chemistry and Physics in Solids*, Chapman and Hall, London, **1973**.
[9] A. Hauser, *Chem. Phys. Lett.* **1992**, *192*, 65–70.
[10] A. Hauser, *J. Chem. Phys.* **1991**, *94*, 2741–2748.
[11] C. P. Köhler, R. Jakobi, E. Meissner, L. Wiehl, H. Spiering, P. Gütlich, *J. Phys. Chem. Solids* **1990**, *51*, 239–247.
[12] A. Hauser, J. Adler, P. Gütlich, *Chem. Phys. Lett.* **1988**, *152*, 468–472.
[13] A. Bousseksou, J. Nasser, J. Linares, K. Boukheddaden, F. Varret, *J. Phys. Sect. I* **1990**, *2*, 1381.